Grid-connected Photovoltaic Micro-inverter with New Hybrid Control LLC Resonant Converter

Xingkui, Mao; Qisheng, Huang; Qingbo, Ke; Yudi, Xiao; Zhang, Zhe; Andersen, Michael A. E.

Published in:
Proceedings of 42nd Annual Conference of the IEEE Industrial Electronics Society

Link to article, DOI:
10.1109/IECON.2016.7793632

Publication date:
2016

Document Version
Peer reviewed version

Grid-connected Photovoltaic Micro-inverter with New Hybrid Control LLC Resonant Converter

Abstract—A high-efficiency photovoltaic (PV) micro-inverter consisting of two power stages i.e. a LLC resonant converter with a new hybrid control scheme and a dc-ac inverter is proposed, studied and designed in this paper. In the first power stage, the new hybrid control combining pulse-frequency modulation (PFM) and phase-shift pulse-width modulation (PS-PWM) is employed on a full-bridge LLC dc-dc converter, in order to achieve high efficiency when PV output voltage varies in a wide range. Moreover, a maximum power point tracking (MPPT) method based on power perturbation is implemented in the dc-ac inverter. Therefore, the complexity of regulating LLC converter can be reduced effectively, and efficiency optimal design can be carried out through the proposed designing procedure for the resonant tank of LLC converter. Finally, a prototype of the proposed PV micro-inverter (PVMI) is developed with rated power of 250W and output voltage of 220VAC/50Hz. The experiment shows that the peak efficiency of the PVMI is 95.5%, where efficiency of LLC converter is up to 97.7%, and the MPPT accuracy is more than 99%.Thus the validity of the proposed system structure, design and control method is verified

Keywords—Photovoltaic micro-inverter; LLC resonant converter; PFM; phase-shift PWM; MPPT

I. Introduction

Nowadays, the PV generation configurations can be classified into central-inverter structure, string-inverter structure and AC-module structure. The central- and string-inverter structures are used for medium- and high-power PV generation whereas the AC module inverters are connected with each PV panel, a so-called micro-inverter, having output power no more than 300W normally [1], [2]. Compared with the other two configurations, advantages like capability against partial shadow, flexibility, and convenience for enlarging capacity appear in AC module [3], [4]. And energy yield of the AC-module is also higher than that of the two other configurations because of its higher utilization of PV panel, although its PVMI has lower efficiency. In [5] it is implied that the generated energy from AC module equipped with micro-inverter is 14% higher than that of centralized structure. But because the PVMI has low and wide-range input voltage, and using isolated topology, it will meet more challenge of achieving high efficiency and high step-up ratio [6-9].

A grid-connected PVMI with a new hybrid control LLC resonant converter is proposed in this paper in order to obtain both efficient conversion and high step-up ratio under wide-range input voltage. This paper is structured as follows. After this Introduction, Section II presents the proposed PVMI configuration, hybrid control method for LLC resonant converter, and MPPT implementation. Section III describes the design of key parameters and simulations. Section IV presents a prototype with rated power of 250W, which is able to adapt to the wide-range input voltage well. Finally the conclusion is given in Section V.

II. Configuration and control of PVMI

2.1 *System configuration*

The proposed PVMI is illustrated in Fig.1. The power circuit consists of two high-frequency power stages. The first power stage DC/DC converter uses full-bridge LLC resonant converter with voltage-doubler rectifier to boost the low and variable input PV voltage into high DC bus voltage, which is controlled with the new hybrid PFM and PS-PWM. The second power stage of a dc-ac inverter inverts the DC bus voltage into grid AC voltage, which is controlled with the dead-beat scheme [10].

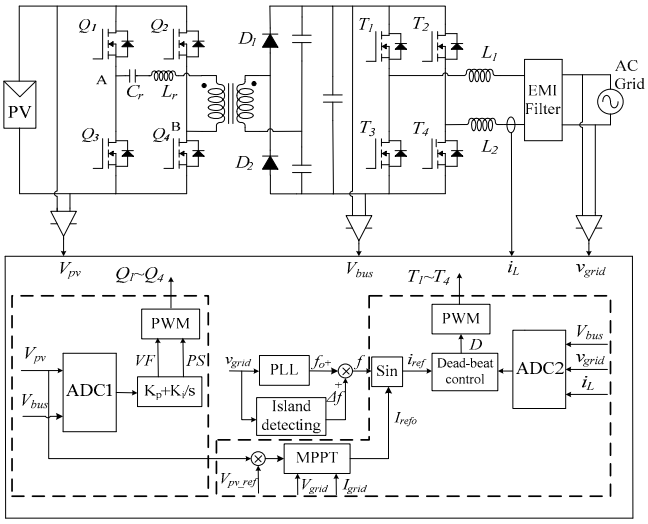

Fig.1 System block diagram of PVMI

In this PVMI, the perturb and observation method is adopted and applied to the second stage dc-ac inverter to

implement MPPT [7]. The high DC bus voltage, acting as output of full bridge LLC resonant converter, is maintained constant with the hybrid control by using PV panel voltage V_{pv} and bus voltage V_{bus}. The reference of injected grid current is obtained via MPPT by using the grid root mean square (RMS) voltage V_{grid}, the injected grid RMS current I_{grid}, and V_{pv}. Moreover, anti-islanding protection can be also achieved by the phase-lock logic (PLL) and active frequency drift with positive feedback (AFDPF) [11]. The ac current with low total harmonic distortion (THD) is obtained through dead-beat control by using V_{bus}, grid instantaneous voltage v_{grid}, and inductor current i_L.

2.2 *Hybrid control for full bridge LLC resonant converter*

Zero voltage switching (ZVS) for the primary side switches and zero current switching (ZCS) for the secondary side diodes can be realized via resonance existing in LLC resonant converter. As shown in Fig. 2, vertical and horizontal axis represents the switching frequency f_s, and the phase-shift duty cycle D respectively. Power can be converted efficiently under narrow-range input voltage with control I i.e. traditional PFM, where the voltage gain is only regulated with f_s [6, 7]. Great challenges in magnetic components, system control, and system stability occur when applying control I to PV panels because of the wide-range switching frequency resulted from wide-range input voltage of PV panel and wide-range load variation. Efficient power conversion under wide-range input voltage can be realized through applying control II. As depicted in Fig.2, PFM is adopted in a region where f_s is smaller than a specific value, while higher f_s for regulation is needed, PS-PWM is used , and so f_s range is limited. The efficiency, however, will decrease under PS-PWM on occasions of high input voltage or light load due to the large D which tending to result in the increases of internal circumfluent current loss.

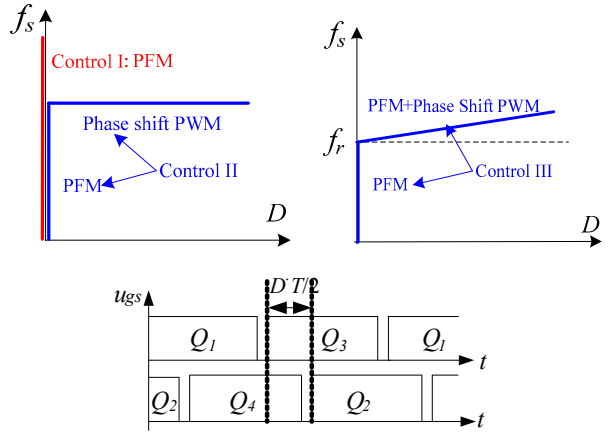

Fig.2 Control scheme for full-bridge LLC resonant converter

In order to overcome the drawbacks by adopting control methods I and II, here a new hybrid control (control III) for full bridge LLC resonant converter is proposed. In control III , there is two control mode. One is PFM control mode when converter $f_s \le$ resonant frequency f_r (fr is resonant frequency of the LLC converter resonant tank, and $f_r = 1/2\pi\sqrt{L_r C_r}$), the other is control mode of combining PFM and PS-PWM (PFM+PS-PWM) when $f_s > f_r$. Here the f_r is selected as frequency for transition of the two control mode, and the converter f_s is designed to be equal to f_r at nominal input voltage and output load working condition. Because PFM is also introduced to combine PFM+PS-PWM for regulation, D will be reduced. Then not only the frequency range is limited effectively in favor of magnetic components design, system control and EMC filtering etc., but also the circumfluent current loss can be decreased because of small D . The new hybrid control scheme can be realized easily with digital control

Considering relatively small D, the voltage gain M of the full bridge LLC converter operating under PFM+PS-PWM control mode can be described as the following equation by using fundamental wave analysis:

$$M(f_S, D, k, Q) = \frac{\sin\frac{D'\pi}{2}}{\sqrt{\left[(1-\frac{1}{f_s^2})\frac{1}{k}+1\right]^2+\left[(f_s-\frac{1}{f_s})\cdot\frac{2}{1-\cos(D'\pi)}Q\right]^2}} \quad (1)$$

Where D′=1-D, k=magnetizing inductance L_m/L_r, Q is the quality factor of the resonant tank. The M acts as the function of f_s and D. k and Q are fixed with the constant parameters of the resonant tank. It is noted that the voltage gain M in Equation (1) will be equal to that of traditional control I when D=0 i.e. no combining PS-PWM. So, the Equation (1) is also the M expression for the PFM control mode via setting D =0.

The PFM control mode can be realized the same like that of traditional PFM. In order to get a specific voltage gain, there exsits a variety of combinations f_s and D under PS-PWM+ PFM mode. The combination guideline can be analyzed according to Equation (1). Because the PFM+ PS-PWM control mode is introduced at $f_s > f_r$, and at $f_s > f_r$ the voltage gain M is less than 1, the following analysis will be only considered at M<1. Normalized switching frequency f vs. Q and D at different M is shown in Fig.3. Here defining $f=f_s/f_r$, and "f>1" means that the LLC converter operates under PS-PWM+ PFM control mode. It is can be seen that,

1. $\Delta f1 < \Delta f2$, which means the range of switching frequency is limited more effectively at small M. In other words, impact resulted from introduction of PS-PWM control on switching frequency is enhanced under high input voltage.

2. The effect of PS-PWM on limiting switching frequency will be weakened with the increases of Q. It means PFM control performs better than PS-PWM control under heavy loads.

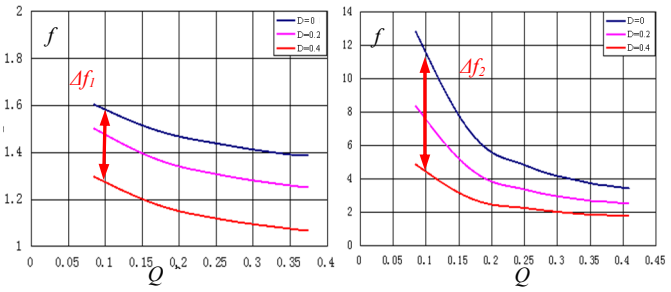

(a) M=0.8 (b) M=0.55

Fig.3. f vs. Q and D @ k=3.7 under PFM+PS-PWM mode

Therefore, the combination guidelines of PS-PWM+ PFM control mode is that introducing large weight for PS-PWM under high input voltage or light load, and large weight for PFM under relative high input voltage or heavy load. Large weight for PS-PWM means that the converter is regulated mainly by PS-PWM and mainly by PFM vice versa. This combination can achieve good trade-off range limitation of between switching frequency and D.

The program flowchart of the hybrid control is shown in Fig.4, which is described step-by-step as following. The output voltage V_{bus} of the LLC resonant converter is compared with the reference voltage in analog to digital (AD) interrupt; thus obtain error V_{error}. The converter will be controlled with PFM if the new calculated switching frequency f_s through PI controller is smaller than resonant frequency f_r. If not, the PS-PWM+PFM control mode will be activated. Then a modification of phase-shift duty cycle ΔD can be calculated according to frequency error which equaling to the differences between f_s and f_r. Finally, f_s and D will be updated by adding ΔD to a reference phase-shift duty cycle D_{base} which had been pre-stored in the register.

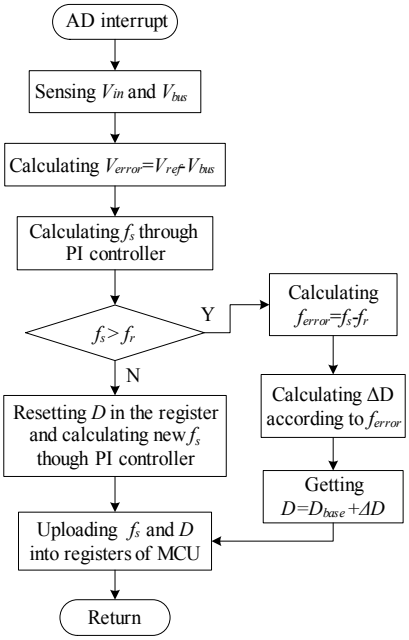

Fig.4 Program flowchart of LLC converter with hybrid control

2.3 MPPT control

Maximum power point tracking (MPPT) is necessary due to the existence of the maximum output power point in PV panel. Method of perturb and observation, which is classified into the first-stage perturbation and the second-stage perturbation, has wide applications [6] on account of its simplicity and high tracking accuracy. Compared with only PFM or PS-PWM, the hybrid control LLC resonant converter has not only two operation mode, but also two control variables f_s and D under PS-PWM+PFM mode. In order to simplify MPPT control, Perturb and observation method is adopted and applied to the second stage dc-ac inverter to implement MPPT. So, the first power stage LLC resonant converter is only controlled to maintained constant output voltage $V_{bus.}$ In order to avoid high sensing loss resulted from low voltage and high current output of PV panel, the perturbing power for MPPT is calculated from sensing grid V_{grid} and $I_{grid,}$ instead of PV output current .

III. Design of key parameters and simulation

3.1 Design of resonant tank of LLC converter

The resonant tank design of LLC resonant converter has impacts on voltage gain, switching losses, and magnetic losses. Minimizing loss is the objective of designing the resonant tank on basis of analyzing the effect of resonant tank parameters on voltage gain and losses. Switches' conduction loss and turn-off loss together are predominated. They are determined by RMS current I_{Q_rms} and turn-off current i_{Q_off}, respectively. Moreover, I_{Q_rms} can also be used to evaluate the magnetic losses.

As shown in Fig.5, $I_{Q\_rms}^*$, $i_{Q\_off}^*$ vs. k and Q in the LLC resonant converter operating PFM mode with f=0.8 are plotted, respectively. Here I_{Q_rms} and i_{Q_off} are normalized as $I_{Q\_rms}^*$ and $i_{Q\_off}^*$. It is shown that large k and Q will achieve small currents, then resulting in the low switches loss. And M will be decreased with increasing of k and Q, resulting in wider switching frequency range. Under PFM+PS-PWM mode, the currents behavior is the same like that of PFM mode. In contrast, its M will be increased with increasing of k, as shown in Fig.6. That is to say, large k will not result in wider switching frequency range. Therefore, in the design k and Q of resonant tank, only effect of k and Q on M under PFM control mode is considered.

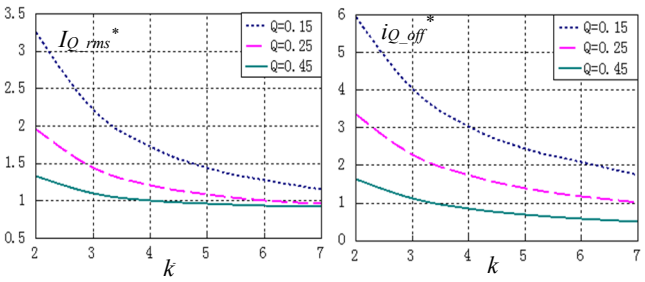

Fig.5 $I_{Q\_rms}^*$, $i_{Q\_off}^*$ vs. k and Q under PFM mode and f=0.8

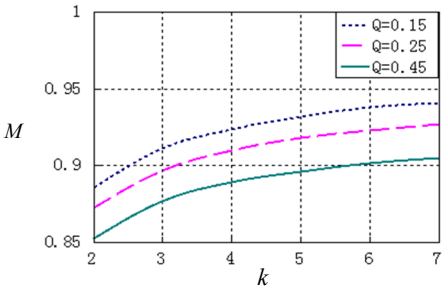

Fig.6 M vs. k and Q under PFM+ PS-PWM mode

The magnetizing current decreases effectively with larger L_m, which is proportional to the multiplication of k and Q, resulting in losses reduction in the resonant network. According to the above conclusion, rules which should be followed in design of the resonant tank are summarized as maximizing the multiplication of k and Q for minimizing losses in resonant network under meeting voltage gain.

Therefore, requirements in the design the LLC converter can be listed as following:

1. Requirements of voltage gain:

$$M(f_{min}) \geq M_{max} \tag{2}$$

$M(f_{min})$ represents the voltage gain at the minimum frequency f_{min}, while M_{max} is the maximum voltage gain under the whole ranges of input voltage and load.

2. Input impedance of the LLC converter need to be inductive in order to operate primary side switches under ZVS. In other words, Im(Z_{in}) must be greater than zero, where Z_{in} represents the input impedance of the converter. Therefore,

$$\omega_s L_r - \frac{1}{\omega_s C_r} + \frac{R_{ac}^2 \cdot \omega_s L_m}{R_{ac}^2 + (\omega_s L_m)^2} > 0 \tag{3}$$

Frequency making the left term of Inequality (3) equal to zero is normalized to be termed as f_{Im_0}, then an inductive Z_{in} can be obtained only when inequality (4) is satisfied.

$$f_{min} > f_{Im\_0} \tag{4}$$

$$f_{Im\_0} = \sqrt{\frac{k^2Q^2 - k - 1 + \sqrt{(k^2Q^2 - k - 1)^2 + 4k^2Q^2}}{2k^2Q^2}}$$

k and Q, shown as overlapped parts in Fig.7, satisfies both Inequality (2) and (4) . Then finding k and Q to maximize the multiplication of k and Q can achieve optimal design.

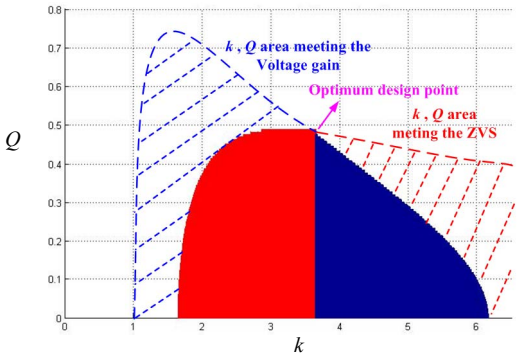

Fig.7 k, Q area meeting the voltage gain and ZVS

According the design procedure, key parameter is designed to be listed as follows for a PVMI prototype.

PV panel voltage: 22-45V/nominal voltage 31V;
MPPT voltage: 25-39V;
PVMI output: 250W /220V (+10%, -15%)/ 50Hz (±0.5Hz);
The LLC resonant converter:
Output voltage or bus voltage V_{bus}= 380V;
Switching frequency f_s: 47k-110kHz, and f_r=65kHz.
Parameters of resonant tank:
k=3.7, Q=0.48, L_r=5.7uH (core size PQ32/25D, material TPW33), C_r=1.1uF, L_m=21uH, turns ratio of transformer: 7:44 (core size EER404513A, material TPW33);
The dc-ac inverter:
Switching frequency: 40kHz for T3,T4; 50Hz for T1,T2;
Inductance: L_1=L_2=2.5mH (core size PQ32/25D, material TPW33).

3.2 Modeling and simulation

Using the control scheme and design parameters, simulations of the PVMI are carried. Some key waveforms are shown in Fig.8. v_{gs}, v_{ds}, i_D, v_D, v_{AB}, i_{Lr} represent drive signal of MOSFET, voltage across drain and source, current and voltage of rectifier diode, voltage across A and B in Fig.1, current of resonant inductor, respectively. It is can be seen that, the LLC converter operates with resonant frequency of 65.5 kHz at nominal input voltage 31V and full-load, while operates with PFM+PS-PWM mode, and f_s= 83.8 kHz, D≈0.2 at input voltage of 39V and full-load. The switching frequency ranges from 47.3 kHz to 111 kHz. The MOSFETs operate with ZVS under full input voltage and loads. It should be noted that ZCS for the diodes, which is in favor of suppressing voltage spike, is also achieved even when f_s is higher than f_r. The reason is that the diodes current lead because of phase shift. This ZCS behavior is great different with that under single PFM control .The simulation has good agreement with the design.

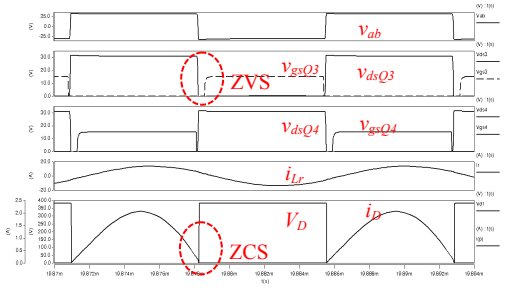

f_s=65.5kHz@ input voltage 31V (under PFM mode)

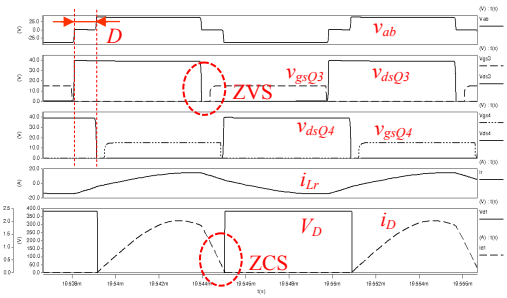

f_s=83.8kHz @ input voltage 39V (under PFM +PS-PWM mode)

Fig.8.Key waveforms of LLC converter vs. input voltage

IV. Experimental results

4.1 *Full-bridge LLC resonant converter*

With the design parameters given in the "section 3.1", the inverter prototype was constructed. Moreover the inverter Q1-Q4 selects Infineon BSC016N06NS and T1-T4 selects IPD60R600C6. And D1, D2 selects STTH5L06. The key waveforms of the full-bridge LLC resonant converter vs. input voltage are given in Fig.9. It is shown that the converter operates with f_s=f_r at nominal input voltage 31V and full load.

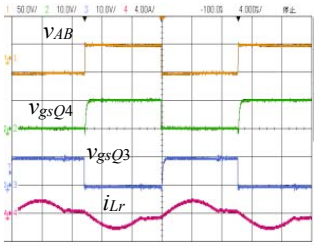

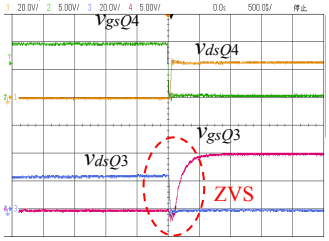

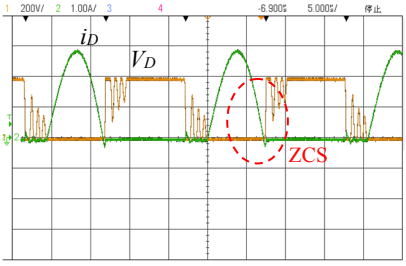

fs = 49.1kHz @ input voltage V_{pv}= 25V, output power P_o=250W

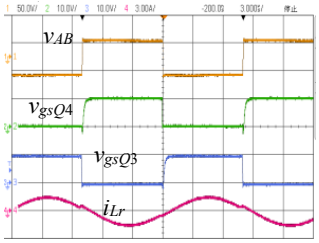

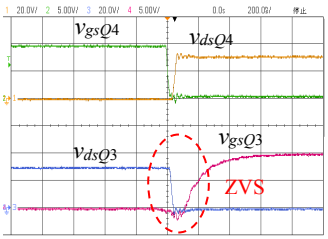

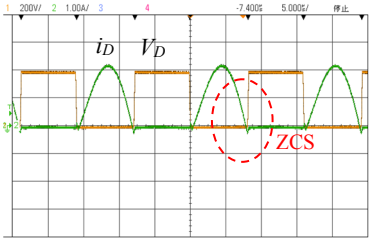

f_s =63.6kHz @ input voltage V_{pv}= 31V, output power P_o=250W

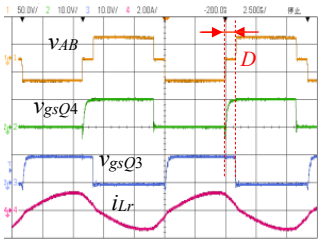

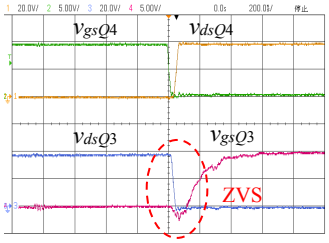

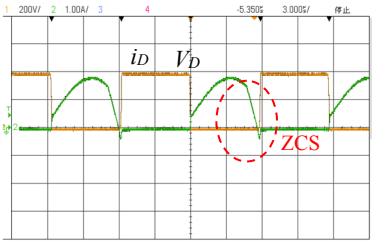

f_s = 87.1kHz @ input voltage V_{in}= 39V, output power P_o=250W

Fig.9 Key waveform of full-bridge LLC converter vs. V_{in}

And the converter operates under PFM control mode when f_s is lower than f_r , while operates at PFM+PS-PWM control mode

As shown in Fig.10, efficiency of the full bridge LLC converter is above 96% within MPPT voltage range from 25 to 39V and peak efficiency is high up to 97.7%.

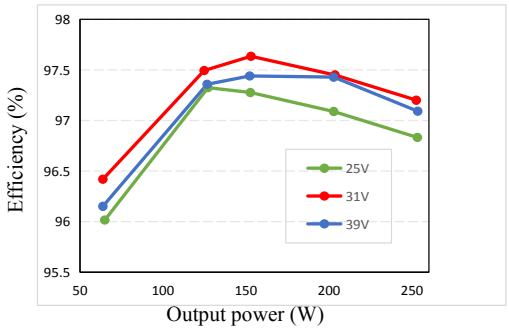

Fig.10 Efficiency of the LLC converter *vs*. V_{pv} and P_o

4.2 *PVMI prototype*

The grid-connected current waveform and its THD, PF are given in Fig.11. The THD is equal to 1.5% at full-load, and equal to 2% at half-load. The efficiency is shown in Fig.12, and the peak efficiency is up to 95.5% at about half-load. The test shows that the prototype has good performance in injected current and efficiency. It should be noted that power consumption 1.45W of auxiliary power supply for the control and drive in the inverter was also included in the test, and this consumption takes up more than 1% of the half-load with peak-efficiency occurring

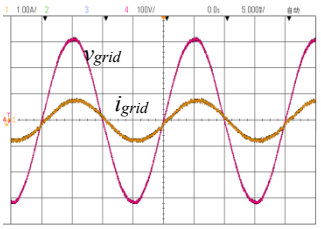

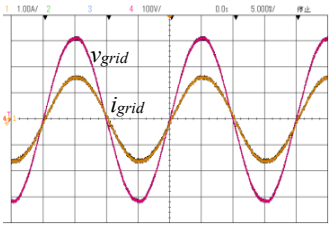

@ Output power half-load 125W @ Output power full-load 250W

(a) Current waveform

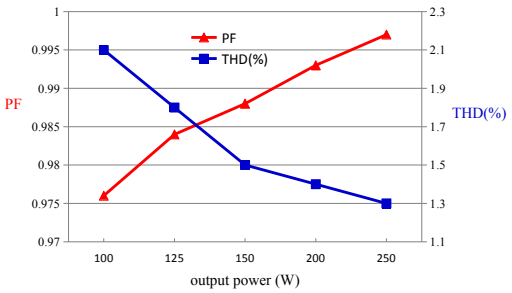

(b) THD and PF of injected current

Fig.11 Injected current @ V_{pv}=31V, v_{grid}=220Vac

The MPPT key waveforms are given in Fig.13. Under the test, the Regatron TCP.16.800.400.PV is used as PV simulator. The maximum power point is set to P_{MP}=250W and V_{MP}=36V. v_{PV}, i_{PV} , p_{PV} is output voltage, current and power of the

simulator, and i_{grid} is the injected current of the inverter. The test shows that the inverter can search to the maximum power point quickly, and has good MPPT accuracy up to 99.3%.

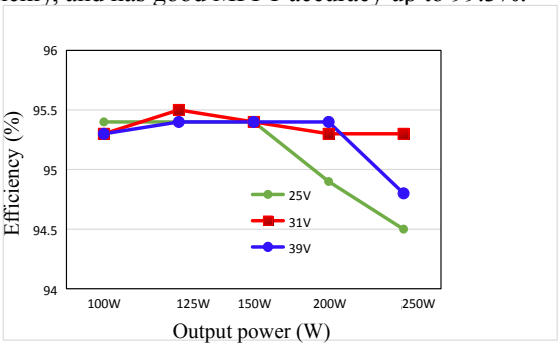

Fig.12 efficiency of the PVMI *vs*. V_{pv} @ v_{grid}=220Vac

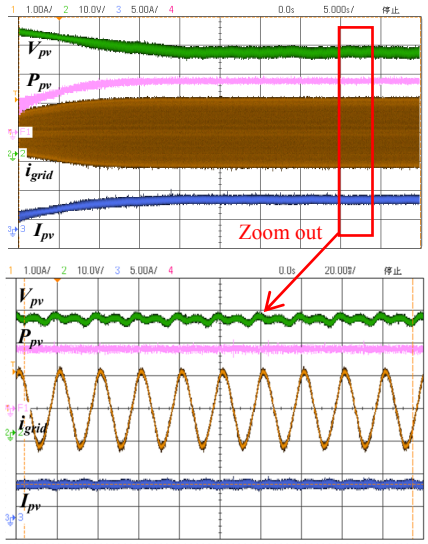

Fig. 13 MPPT key waveform @ P_{MP}=250W, V_{MP}=36V

V. Conclusion

The PVMI will meet more challenge of achieving high efficiency because of wide-range input voltage, A PVMI with two high-frequency power stages is proposed, and the full bridge LLC resonant converter with hybrid control is used for the first power stage to meet PV wide range input voltage. The LLC resonant converter operates PFM mode when switching frequency is lower than the resonant frequency; otherwise, it operates with combining PFM and phase-shift PWM mode instead. Therefore, not only switching frequency range is limited, but also circumfluent current loss is decreased due to the reductions of phase-shift duty cycle under this proposed hybrid control. MPPT control is implemented on the second stage in order to avoid large amount of control variables existing in the LLC converter. Efficiency optimal design is implemented through the proposed design procedure for the resonant tank. Finally the experimental results verify the validity of the proposed scheme, design and control method.

REFERENCES

[1] S. B. Kjaer, and John K. P., "A review of single-phase grid- connected inverters for photovoltaic modules", *IEEE Trans. on I. A.*, vol.41, no.5, pp.1292-1305, Oct. 2005.

[2] Quan Li, and Peter Wolfs, "A review of the single phase photovoltaic module integrated converter topologies with three different DC link configurations", *IEEE Trans. on P.E*, vol.23,no.3, pp.1320-1333, May 2008.

[3] T. Freddy, N. A. Rahim, et al., "Comparison and analysis of single-phase transformerless grid-connected PV inverters" , *IEEE Trans. on P.E,* vol. 29, no. 10, pp. 5358–5369, Oct. 2014.

[4] H. Hu, et al., "A review of power decoupling techniques for micro-inverters with three different decoupling capacitor locations in PV systems," *IEEE Trans. on P.E.*, vol. 28,no. 6, pp. 2711–2726, Jun. 2013.

[5] A. Elasser, " Photovoltaics systems: overview, status, and future prospects", *IEEE Rensseler Polytechnic Institute PV System Seminar' 2010*, Oct. 2010, pp. 1-45.

[6] Haibing Hu, et al., "A modified high-efficiency LLC converter with two transformers for wide input-voltage range applications", *IEEE Trans. on P.E*, vol.28, no.4, pp.1946-1960, Apr. 2013.

[7] Qian Zhang, et al., "A center point iteration MPPT method with application on the frequency-modulated LLC micro-inverter", *IEEE Trans. on P.E*, vol.29, no.3, pp.1261 -1274, Mar. 2014.

[8] Li Ju, and RuanXinbo, "Hybrid control strategy of full bridge LLC converters", *Trans. of China Electrotechnical Society*, vol.28, no.4, pp.72-79, Apr. 2014.

[9] Wardah Inam, K. K. Afridi, David J. P., "High efficiency resonant DC/DC converter utilizing a resistance compression network", *IEEE Trans. on P.E*, vol.29, no.8, pp.4126- 4135, Aug.2014.

[10] Simone Buso, et al.,"Dead-beat current controller for voltage- source converters with improved large-signal response", *IEEE Trans. on I. A.*, vol.52, no.2, pp. 1588-1596, Mar/Apr. 2016.

[11] Jung Y., et al., "A novel active frequency drift method of islanding prevention for the grid-connected Photovoltaic inverter", in *Proc. PESC*, 2005, pp. 1915–1921.